17th World Conference on Earthquake Engineering, 17WCEE
Sendai, Japan - September 13th to 18th 2020

LIQUEFACTION - INDUCED PROBABILISTIC SEISMIC RISK ASSESSMENT

C. Yilmaz [1], V. Silva [2], G. Weatherill [3]

[1] *PhD. Student Completed, IUSS Pavia, cigdem.yilmaz@iusspavia.it*
[2] *Risk Coordinator, GEM Foundation, Pavia, vitor.silva@globalquakemodel.org*
[3] *Hazard Scientist, GFZ Potsdam, gweather@gfz-potsdam.de*

Abstract

Earthquake-induced ground shaking is the primary cause of the damage to buildings and infrastructure. However, secondary effects such as liquefaction, can also have important consequences. For some earthquakes, liquefaction has been responsible for more than half of the total damage caused by the seismic event (e.g. Alaska, USA – 1964, Niigata, Japan - 1964). Thus, the purpose of this study is to conduct a complete probabilistic liquefaction risk assessment at a large (regional or national) scale. The estimation of the losses with a probabilistic approach requires three main components. The first is the probabilistic seismic hazard assessment model, which allows for the generation of stochastic events sets and estimation of permanent ground displacements (PGD) with the associated probability of occurrence. These calculations are performed using the new geotechnical module of the OpenQuake-engine. The second component is represented by an exposure model, which describes the replacement value, building class and the spatial distribution of the elements exposed to the seismic hazard. The final component comprises the vulnerability functions that establish the distribution of loss ratio for a range of hazard intensities (i.e. PGD). For this study, the second and third components are adopted from existing studies, such as the HAZUS software package and H2020 SERA European project. The probabilistic framework for predicting the losses due to liquefaction is applied to mainland Portugal.

Keywords: Liquefaction, Seismic Risk, Loss Assessment, OpenQuake,

1. Introduction

Seismic risk assessment enables an understanding of the potential damage and losses that may occur due to earthquake. However, most risk assessment methodologies applied in practice do not include the impact of ground failure. The severity of the liquefaction phenomena was observed during the earthquakes in 1964 in Alaska and Japan, in 1995 in Kobe, Japan, in 1999 in Kocaeli, Turkey [1] and in 2011 in Christchurch, New Zealand [2]. These earthquakes demonstrated that in order to provide a complete loss assessment for a region, the contribution of the losses due to liquefaction should not be neglected. On the other hand, although loss assessment studies are mostly applied on a large scale (e.g. regional, national), the available liquefaction methodologies often require a detailed assessment, which can be too expensive, time consuming, and ultimately impractical [3].

In order to fulfil the need for an open tool that can evaluate ground failure hazard and calculate the expected losses at any scale, existing methodologies of ground failure assessment (both for liquefaction and landslide) were introduced into an open module, compatible with the OpenQuake-engine supported by the Global Earthquake Model (GEM) Foundation. The methodologies were selected based on their input parameters, which can be obtained easily. The steps of the framework are respectively the calculation of the permanent ground deformation (PGD), definition of the elements at risk, and the estimation of the building damage due to liquefaction. Portugal was selected as a case study to demonstrate the framework.

2. Simplified Models for the Assessment of Liquefaction Probability

There are many different models to predict the liquefaction potential, however most of them are developed for the single site assessment and require detailed data. For the regional scale liquefaction assessment, the most commonly used models are empirical models, which are based on the easily obtainable parameters. In this study two models are adopted for the assessment of liquefaction probability, one is developed by Zhu et al. [4] and the other one is HAZUS [5].

2.1. Zhu et al. [4]

Zhu et al. [4] proposed an approach to estimate liquefaction potential by using accessible geospatial data as predictor variables, through empirical equations for use in rapid response and loss estimation. To estimate the probability of liquefaction, Zhu et al. [4] used a logistic regression, so that the probability ranges between 0 and 1.

$$PL = \frac{1}{1 + e^{-x}} \tag{1}$$

where x is the linear prediction function of the explanatory variables.

The global linear predictor (X_G) model with simplified explanatory variables is calculated as:

$$X_G = 24.1 + lnPGA + 0.355CTI - 4.784lnV_{S30} \tag{2}$$

where CTI is the compound topographic index, which is a steady-state wetness index used as a proxy for the soil saturation. Due to the relatively easy estimation and simplicity, Zhu et al. [4] suggested using Vs_{30} from slope following the method described in Wald and Allen [6]. This methodology is hereafter termed as Zhu.

2.2. HAZUS [5]

The initial step for liquefaction hazard assessment is to characterize the liquefaction susceptibility of the region, based on the soil/geologic conditions proposed by Youd and Perkins [7]. The liquefaction susceptibility is divided into six classes, ranging from none to very high.

The probability of liquefaction is calculated as a function of the peak horizontal acceleration (PGA), susceptibility class, earthquake magnitude (M_w) and the depth of the groundwater (d_w). Thus, the probability of liquefaction for a given susceptibility category can be determined by the following relationships:

$$P[Liquefaction_{SC}] = \frac{P[Liquefaction_{SC} \mid PGA = a]}{K_M * K_W} * P_{ml} \tag{3}$$

$$K_M = 0.0027{M_W}^3 - 0.00267{M_W}^2 - 0.2055M_W + 2.9188 \tag{4}$$

$$K_W = 0.022d_W + 0.93 \tag{5}$$

here P[PGA=a] is the conditional liquefaction probability for a given susceptibility category, at a specified level of peak ground acceleration. K_m is the moment magnitude correction factor, K_w is the groundwater correction and P_{ml} is the proportion of map unit susceptible to liquefaction. This methodology is hereafter termed as HZ.

3. Simplified Models for the Estimation of Liquefaction- Induced Ground Failures

As it was mentioned in the previous section, also for the estimation of liquefaction-induced ground failure the majority of the models require detailed geotechnical data. From the small number of available approaches in the literature, two models of HAZUS [5] are selected to compute the vertical settlement and lateral spread.

3.1. HAZUS Methodology for the Estimation of Vertical Settlement

Vertical settlement depends on the probability of liquefaction (Eq. (3)) and the expected settlement amplitude, which is related to the susceptibility level. In this methodology, the vertical settlement is dependent only on the susceptibility category, and therefore the degree of settlement is not affected by the strength of the shaking [8].

3.2. HAZUS Methodology for the Estimation of Lateral Spreading

The lateral spreading is calculated as a function of PGA and susceptibility class as follows:

$$E[PGD_{SC}] = K_{\Delta} * E[PGD \mid \left({}^{PGA}/_{PL_{SC}}\right) = a] \quad (6)$$

$$K_{\Delta} = 0.0086M^3 - 0.0914M^2 + 0.4698M - 0.9835 \quad (7)$$

where, $E\left[PGD \mid \left({}^{PGA}/_{PL_{SC}}\right) = a\right]$ is the expected ground displacement for a given susceptibility category under a specified level of normalized ground shaking (PGA/PGA(t)). PGA(t) is the acceleration threshold for a susceptibility category, at which liquefaction can be triggered. K_{Δ} is the displacement correction factor and M_w is the moment magnitude.

4. Description of Case Study and Input Parameters

The seismic hazard of Portugal is characterized by large offshore and moderate onshore earthquakes [9]. Whilst the northern and central part of Portugal are characterized by low seismicity ($M_w < 5$), the Lower Tagus Valley (LTV) region and southern part of Portugal have relatively high seismic activity, such as in 1344 ($M_w > 6$), 1531 ($M_w = 7$), 1722 ($M_w = 7.5$), 1755 ($M_w = 8.5$), 1909 ($M_w = 6.3$), and 1969 ($M_w = 7.8$). Based on the historical liquefaction event database developed by Vaz and Zêzere [10], most of the liquefaction cases occurred in Santarem, Leiria and Coimbra districts (see Fig. 1) [10].

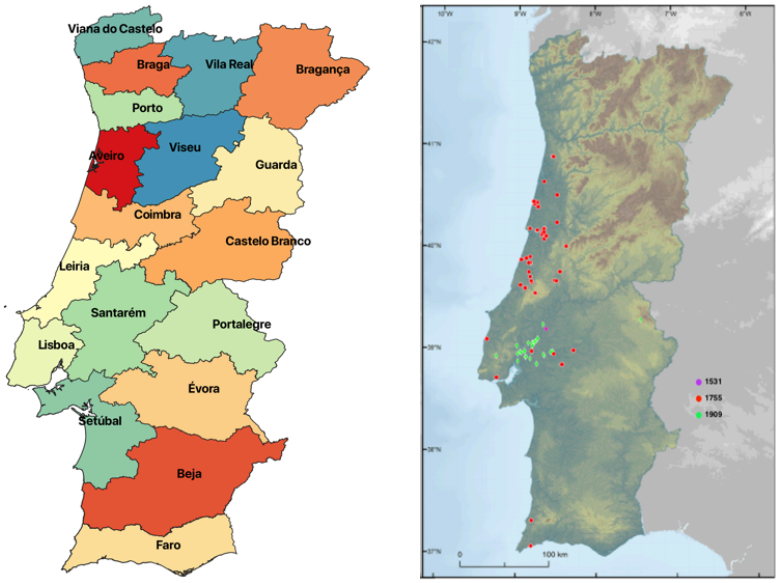

Fig. 1– Regions of Portugal (left) and location of the identified liquefaction (right) [10]

For the implementation of the liquefaction models, the regional geology of Portugal must be defined. To do so, a lithology map of the country is adopted from the OneGeology platform [11]. The Zhu model suggests deriving Vs_{30} values using the topography-based approach [5]. However, in this study the Vs_{30} values were derived following a geology-based methodology [12], as many researches [13, 14, 15, 16] indicated a better correlation between Vs_{30} and geology in comparison with, topography. To determine Vs_{30} values and the HAZUS susceptibility groups, each geological unit was classified into five different groups based on information from NEHRP [17] and the Eurocode 8 (EC8) [18] provisions. The geological structure and Vs_{30} values assigned for each soil category are shown in Table 1.

Table 1- Lithologic groups, definition and Vs_{30} values of the units

Soil Categories	Description of Profile	Geologic Unit	Vs_{30} (m/s)
A	Igneous and metamorphic rocks	Limestone, mica schist, quartzite, gneiss, phyllite, marble	> 760
B	Mesozoic and Paleogene sedimentary rocks	Calcareous sandstone, marl, conglomerate	760 - 520
C	Miocene and Pliocene formations	Sandstone, gypsums, detrital rocks, shales	520 - 360
D	Pleistocene and Holocene formations	Gravel, sand, silt, stiff clay	180 - 360
E	Quaternary soft soils	Mud, alluvium	< 180

The Vs_{30} values and liquefaction susceptibility are verified using the geologic map of Portugal (Fig. 2). The susceptibility map consists of 6 groups ranging from 0 (i.e. none) to 5 (i.e. very high). Very low and low (0-1) potential includes soil classes A and B, moderate (2) susceptibility includes class C, high (4) liquefaction susceptibility consists of soil class D, and finally, very high (5) susceptibility is related with soil class E.

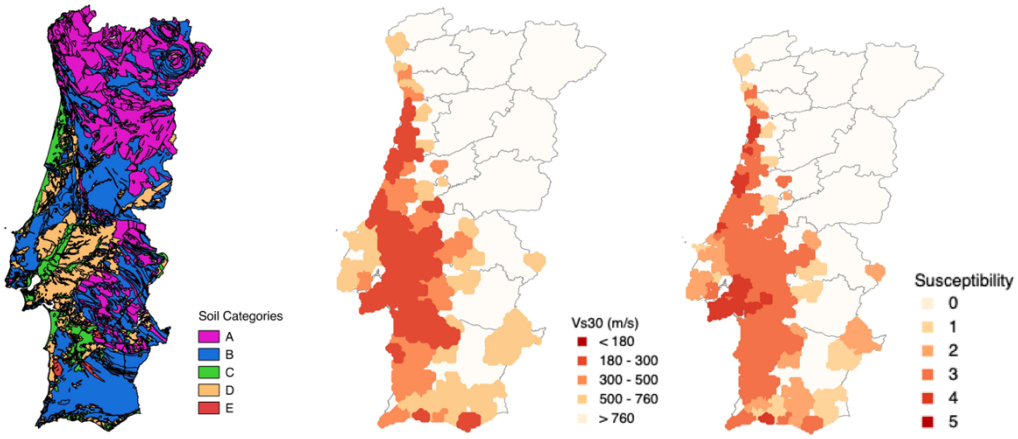

Fig. 2- Geological map (left), Vs_{30} map (middle) and the liquefaction susceptibility map of Portugal

The groundwater depth is derived from a global dataset of water depth by Fan et al. [19]. For the Zhu model, the compound topographic index (CTI) is derived from a Digital Elevation Model (DEM), using the hydrological tools in ArcGIS. The Digital Elevation Model was extracted from the European Environment Agency (EEA) portal [20].

5. Probabilistic Framework for Liquefaction-Induced Risk Assessment

5.1. Probabilistic Seismic Hazard Assessment

The first step in the risk assessment due to liquefaction is the estimation of a hazard intensity, such as permanent ground deformation (PGD). For this purpose, the classical PSHA methodology was extended to the ground deformation using the scalar formulation by Saygili and Rathje [21]:

$$\lambda_D(d) = \lambda_0 \int_z \int_m \int_r P[D \geq d | GM = z] \cdot f_{GM}(z|m,r) \cdot f_m(m) \cdot f_R(r|m) \cdot d_m d_r d_z \quad (8)$$

where $\lambda_D(d)$ represents the mean annual rate that the displacement (D) exceeds the given displacement level d, P [D ≥ d | GM = z] is the probability that the ground displacement level d is exceeded when the input ground motion is equal to z. This is the main additional component in the OpenQuake-engine required to extend classical PSHA to the ground failure hazard computation.

For the risk analysis of the geographically distributed building portfolios, it is appropriate to characterize seismic hazard using a set of joint ground motion and displacement fields generated by seismic scenarios. This requires that for each ground displacement field the corresponding probability of failure should be calculated. Thus, the seismic hazard estimation is performed using the event-based geotechnical calculator within the OpenQuake-engine. The details about the workflow of the geotechnical calculator are described in [22, 23]. To estimate the ground motion parameters, the seismic source model from the European FP7 Project SHARE (Seismic Hazard Harmonization in Europe) model [24] was used.

Due to the time-consuming calculation process, some changes were applied to the SHARE model in order to reduce the number of non-damaging ground motion fields generated. Firstly, out of three source models, only one source model (i.e. area source model - AS-model) was taken into account. Secondly, instead of considering the full logic tree branches, one branch per tectonic regime type was selected. Thus, all of the weights for the source model and GMPEs were set to 1.0. For the event-based probabilistic ground failure calculation, the investigation time was set to 100,000 years.

5.2. Exposure Model

The second component of the seismic loss model is the definition of the elements at risk using an exposure model, which contains the information about the location, number and type of exposed assets, and value or replacement cost. For loss assessment due to liquefaction, one of the most important building attributes is the type of the foundation. However, this attribute is often unknown in common exposure models for large scale risk analysis. Therefore, reasonable assumptions must be made regarding the foundation type [8]. For this study, the residential building exposure models were extracted from the ongoing SERA (Seismology and Earthquake Engineering Research Infrastructure Alliance for Europe) European project [25]. The building stock is considered to be distributed based on the population and night-time lights over an evenly spaced grid with a 5 km by 5 km resolution following the approach described in [26].

5.3. Building Damage Estimation

As the third component of the risk assessment, the vulnerability model from HZ was utilised. This is the only practical model available to estimate building damage due to both vertical settlement and lateral spreading (see Fig. 3). According to HZ, the building damage due to ground failure is characterised by one combined extensive/complete damage state. The P [E or C] describes the probability of exceeding extensive or complete damage for a given permanent ground deformation (PGD). The only difference across different building classes is based on the foundation type, divided between shallow and deep foundations. The fragility curve from HZ is applicable only for buildings on shallow foundations. For the case of structures supported by a deep foundation, the probability of extensive or complete damage is reduced by a factor of 10 for settlement-induced damage, and by a factor of 2 for lateral spreading-induced damage [6].

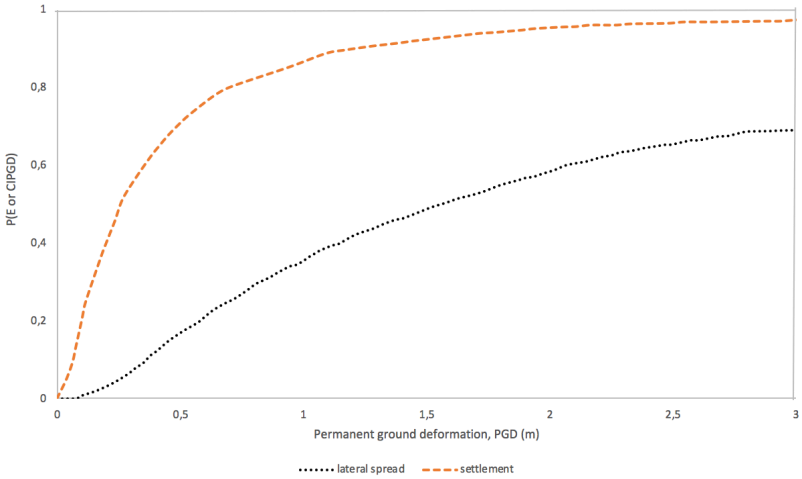

Fig. 3- HAZUS fragility curve for all buildings with shallow foundations

6. Probabilistic Loss Estimation due to Liquefaction

6.1. Probability of Liquefaction Occurrence

The probability of liquefaction indicates at least one liquefaction occurrence in the area. The annual probability of liquefaction is calculated as:

$$P[L] = \sum_i P[L|E_i] \cdot P[E_i] \tag{9}$$

where, P[L | E_i] is the probability of liquefaction occurrence given event E_i, and P[E_i] is the annual probability of seismic event E_i.

Fig. 4 shows the average annual probability of liquefaction occurrence computed with the HZ and Zhu models. The results are consistent with the susceptibility and historical event maps in Fig. 2. Both models indicate that the expected areas of liquefaction are generally located in the western parts of the country (e.g. Santarem, Setubal) and the southern parts (i.e. Faro district), near the coastal zone. The northern and eastern parts of the country have a relatively small probability, due to the low seismicity and stiffer soil formations.

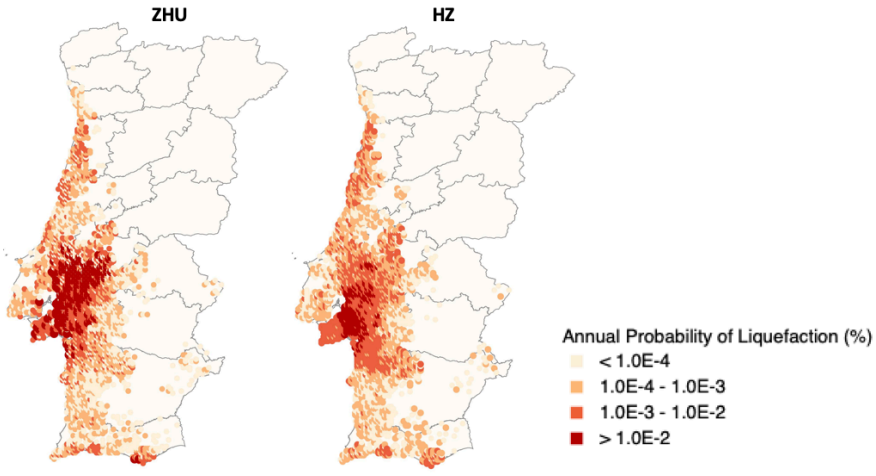

Fig. 4- The annual probability of liquefaction occurrence with the Zhu (left) and HZ (right) models.

6.2. Loss Curves Due to Liquefaction

The losses across the region of interest are summed, leading to an aggregated loss per region. This list of losses can be used to estimate the rate of exceeding a set of loss levels as described in the following expression:

$$\lambda(L > l) = \sum_{i=1}^{j} P(L > l \,|Rup_i).\lambda(Rup_i) \tag{10}$$

where P ($L > l \,|\, Rup_i$) is the probability that a given loss value l will be exceeded for a particular rupture and $\lambda(Rup_i)$ is the annual rate of rupture i. The reason for the probabilistic distribution of loss for a given rupture i (as opposed to a single loss value) is due to the variation in the probability of liquefaction occurrence at each site. This rate can then be transformed into a probability of exceedance assuming a Poissonian distribution [29]. The results are shown in terms of loss exceedance curves, which indicate the relation between the economic loss and the annual frequency of occurrence of that loss [30].

It should be noted that the Zhu model calculates only the probability of liquefaction. In order to extend the probabilities to the displacement calculations, the displacement equations from the HZ were used. Thus, the losses are calculated using the combination of deformation amplitudes from the HZ and liquefaction probabilities from the Zhu model. The loss exceedance curves calculated with the two models are presented in Fig. 5.

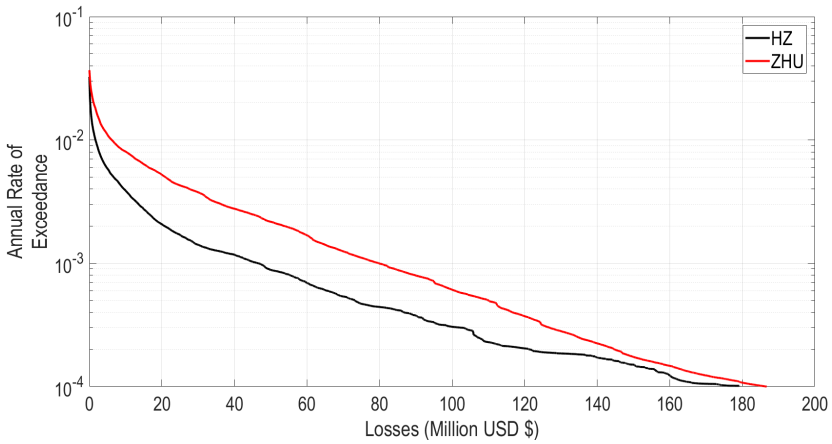

Fig. 5- Loss exceedance curves due to liquefaction

As expected, the losses calculated with the Zhu model are higher than the ones calculated using the HZ approach. This is because the vertical settlement is a function of liquefaction probability and the probabilities estimated with the Zhu model are higher than the ones calculated with the HZ equations.

6.3. Loss Maps due to Liquefaction

The average annualized loss (AAL) can be calculated by summing up the annual losses (AL) from all of the events considering their probability of occurrence (P(AL_i)) and dividing by the investigation time (n) [31]:

$$AAL = \frac{1}{n}\sum_{i=1}^{n} P(AL_i)AL_i \tag{11}$$

In Fig. 6 the AAL maps at the first administrative level are presented. As expected, the losses with the ZHU model are higher than the HZ model. The results show that the losses in Santarem and Setubal districts are relatively higher than the other districts. Moreover, contrary to the hazard potential, Lisbon can have considerable losses due to the higher building density. In Portugal, most of the buildings are assumed to have a shallow foundation system, which exacerbates the potential losses due to liquefaction.

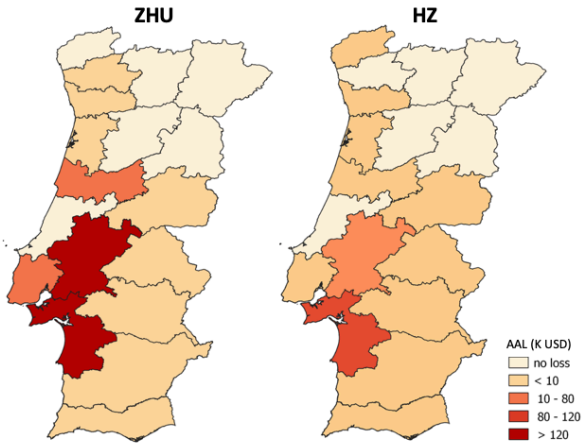

Fig. 6- Annual average loss due to liquefaction calculated with the Zhu (left) and HZ (right) models

8. Conclusion

Earthquake-induced liquefaction can have an important contribution to the earthquake induce losses of building portfolios. There are well established tools and models for the determination of liquefaction potential and induced ground displacement at the local scale, however their evident shortcomings complicate their applications on regional probabilistic loss assessment. Therefore, a tool using the OpenQuake-engine was built to estimate losses caused by secondary hazards for large-scale risk analyses, and the adopted methodologies for liquefaction assessment are applied to determine the potential liquefaction-induced losses in Portugal.

Two models were explored for liquefaction potential. Each model has been developed using different datasets and following different assumptions, therefore there are some differences in their estimations. The Zhu model considers two parameters related to soil, the soil density (Vs_{30}) and the degree of saturation (CTI), while the HZ model considers only the ground water depth. Also, the susceptibility classes are based on the subjective decisions, which influence the model estimations significantly. Moreover, in the calculation of liquefaction probability, HZ model uses the proportion of map unit (P_{ml}) parameter, which saturates the liquefaction probability to 25%, even for soils that are very highly susceptible to liquefaction [1]. Therefore, due to its parameters and assumptions, the HZ model may underestimate the liquefaction potential.

For the calculation of the permanent ground deformations (e.g. vertical settlement and lateral spread), the models from HZ approach were adopted. The displacement calculations require the probability of occurrence. Thus, the HZ displacement values were combined with the probability values from the HZ approach and the Zhu model, which renders the loss calculations with two different approaches possible.

The results show that the liquefaction potential of Portugal is consistent with the historical events. More specifically, the liquefaction hazard potential and the average annual losses are mainly concentrated in the western region. Despite the low liquefaction hazard in the city of Lisbon, the estimated losses are considerable due to the large building concentration on shallow foundations.

9. References

[1] Bird JF, Bommer, JJ (2004): Earthquake losses due to ground failure. *Engineering Geology*, **75**, 147-179.

[2] Cubrinovski M, Taylor M, Henderson D, Winkley A, Haskell J, Bradley BA, Hughes M, Wotherspoon L, Bray J, O'Rourke T (2014): Key factors in the liquefaction-induced damage to buildings and infrastructure in Christchurch: Preliminary findings. *New Zealand Society for Earthquake Engineering Annual Conference (NZSEE).*

[3] Kongar I, Rossetto T., Giovinazzi S. (2015): Evaluating Desktop Methods for Assessing Liquefaction-Induced Damage to Infrastructure for the Insurance Sector. *12th International Conference on Applications of Statistics and Probability in Civil Engineering, ICASP12*, Vancouver, Canada.

[4] Zhu J, Daley D, Baise L, Thompson E, Wald D, Knudsen K (2015): A Geospatial Liquefaction Model for Rapid Response and Loss Estimation. *Earthquake Spectra*, **31** (3), 1813-1837.

[5] NIBS (2003): *HAZUS-MH Technical Manua*l, NIBS (National Institute of Building Sciences), Washington, D.C.

[6] Wald D, Allen T (2007): Topographic slope as a proxy for seismic site conditions and amplification. *Bulletin of the Seismological Society of America*, **102**, 169-184.

[7] Youd TL, Perkins, DM (1978): Mapping liquefaction- induced ground failure potential. *Journal of Geotechnical Engineering*, **104** (4), 433-446.

[8] Bird JF, Crowley H, Pinho R, Bommer JJ (2005): Assessment of building response to liquefaction induced differential ground deformation. *Bulletin of the New Zealand Society for Earthquake Engineering*, **38** (4), 215-234.

[9] Moreira VS (1989): Seismicity of the Portuguese Continental Margin. In: Earthquakes at North-Atlantic Passive Margins: Neotectonics and Postglacial Rebound," *NATO ASI Series (Series C: Mathematical and Physical Sciences)*, Vol. 266. Springer, Dordrecht.

[10] Vaz T, Zêzere JL (2016): Landslides and other geomorphologic and hydrologic effects induced by earthquakes in Portugal. *Natural Hazards*, **81**, 71–98.

[11] OneGeology: http://www.europe-geology.eu/onshore-geology/geological-map/onegeologyeurope/

[12] Wills C J, Clahan KB (2006): Developing a map of geologically defined site condition categories for California. *Bulletin of the Seismological Society of America*, **96**, 1483-1501.

[13] Lemoine A, Douglas J, Cotton F (2012): Testing the applicability of correlations between topographic slope and V_{S30} for Europe. *Bulletin of the Seismological Society of America,* **102**, 2585–2599.

[14] Pilz M, Parolai S, Picozzi M, Wang R, Leyton F, Campos J, Zschau J (2010): Shear wave velocity model of the Santiago de Chile basin derived from ambient noise measurements: a comparison of proxies for seismic site conditions and amplification. *Geophysical Journal International*, **182**, 355–367.

[15] Stewart JP, Klimis N, Savvaidis A. Theodoulidis N, Zargli E, Athanasopoulos G. Pelekis P, Mylonakis G, Margaris B (2014): Compilation of a local VS profile database and its application for inference of V_{S30} from geologic-and terrain-based proxies. *Bulletin of the Seismological Society of America,* **104**, 2827–2841.

[16] Vilanova S, Narciso J, Carvalho J, Lopes I, Quinta-Ferreira M, Pinto C, Moura R, Borges J, Nemser ES (2018) "Developing a Geologically Based V_{S30} Site-Condition Model for Portugal: Methodology and Assessment of the Performance of Proxies. *Bulletin of the Seismological Society of America*, **108** (1), 322-337.

[17] Building Seismic Safety Council (BSSC) (2003): NEHRP Recommended Provisions for seismic Regulations for New buildings and other Structures, Part1: Provisions. *Federal Emergency Management Agency (FEMA)*, Washington, D.C.

[18] CEN (2004): Eurocode 8—design of structures for earthquake resistance. Part 1: general rules, seismic actions and rules for buildings. *European standard EN 1998-1*, European Committee for Standardization, Brussels

[19] Fan Y, Li H, Miguez-Macho G (2013): Global patterns of groundwater table depth", *Science*, **339** (6122), 940-943.

[20] European Environment Agency (EEA) portal: https://www.eea.europa.eu/data-and-maps/data/eu-dem/

[21] Saygili G, Rathje EM (2008): Empirical predictive models for earthquake-induced sliding displacements of slopes. *Journal of Geotechnical and Geoenvironmental Engineering* **134** (6), 790–803.

[22] Weatherill G, Yilmaz C, Silva V (2019): Using OpenQuake for probabilistic hazard and risk assessment of seismically-induced ground displacements: Lessons learned from implementation and consideration for application. *Proceedings of 7th International Conference on Earthquake Geotechnical Engineering (7ICEGE), Rome, Italy*

[23] Yilmaz C (2019): Probabilistic Loss Assessment Due to Earthquake- Induced Ground Failure. *PhD Thesis*, Understanding and Managing Extremes (UME) School, IUSS Pavia, Italy

[24] European Facility of Earthquake Hazard and Risk (EFEHR): www.efehr.org

[25] The Seismology and Earthquake Engineering Research Infrastructure Alliance for Europe (SERA): www.sera-eu.org

[26] Silva V, Crowley H, Varum H, Pinho R (2015): Seismic Risk Assessment for Mainland Portugal. *Bulletin Earthquake Engineering*, **13** (2), 429-457.

[27] Hunter GJ, Goodchild MF (1997): Modelling the Uncertainty of Slope and Aspect Estimates Derived from Spatial Databases. *Geographical Analysis*, **29** (1), 35-49.

[28] Wills C, Gutierrez C, Perez A, Branum D (2015): A Next Generation V S 30 Map for California Based on Geology and Topography. *Bulletin of the Seismological Society of America*, **105** (6), 3083.

[29] Crowley H (2005): An Investigative Study on the Modelling of Earthquake Hazard for Loss Assessment. *Individual Study*, European School for Advanced Studies in Reduction of Seismic Risk (ROSE School), University of Pavia, Italy.

[30] Velásquez CA, Cardona O, Yamin L, Mora M, Tibaduiz M, Barbat A (2013): Hybrid loss exceedance curve (HLEC) for risk assessment. *International Symposium on Computational Civil Engineering, Romania*.

[31] Silva V (2016): Critical Issues in Earthquake Scenario Loss Modelling. *Journal of Earthquake Engineering*, **20** (8), 1322-1341.

